CONTRASTIVE WEAK-TO-STRONG GENERALIZATION

Anonymous authorsPaper under double-blind review

000

001 002 003

004

006

008 009

010

011

012

013

014

015

016

017

018

019

021

024

025

026

028 029

031

033

034

037

040

041

042

043

044

046

047

048

051

052

ABSTRACT

Weak-to-strong generalization provides a promising paradigm for scaling large language models (LLMs) by training stronger models on samples from aligned weaker ones, without requiring human feedback or explicit reward modeling. However, its robustness and generalization are hindered by the noise and biases in weak-model outputs, which limit its applicability in practice. To address this challenge, we leverage implicit rewards, which approximate explicit rewards through log-likelihood ratios, and reveal their structural equivalence with Contrastive Decoding (CD), a decoding strategy shown to reduce noise in LLM generation. Building on this connection, we propose Contrastive Weak-to-Strong Generalization (ConG), a framework that employs contrastive decoding between pre- and post-alignment weak models to generate higher-quality samples. This approach enables more reliable capability transfer, denoising, and improved robustness, substantially mitigating the limitations of traditional weak-to-strong methods. Empirical results across different model families confirm consistent improvements, demonstrating the generality and effectiveness of ConG. Taken together, our findings highlight the potential of ConG to advance weak-to-strong generalization and provide a promising pathway toward AGI. Our code is available at: https://anonymous.4open.science/r/ConG/

1 Introduction

Weak-to-strong generalization has emerged as a promising paradigm for scaling the capabilities of large language models (LLMs) (Burns et al., 2024; Yao et al., 2025; Li et al., 2025; Somerstep et al., 2025; Zhou et al., 2024b). By leveraging supervised samples generated from an aligned weaker model, a stronger model can be directly trained without requiring additional reward modeling or human feedback (Burns et al., 2024; Ouyang et al., 2022; Lee et al., 2024). This enables LLMs to transfer and extend capabilities to even stronger models, providing opportunities for self-enhancement and thus offering a potential pathway toward Artificial General Intelligence (AGI) (Goertzel, 2014).

Despite encouraging progress, the paradigm suffers from poor robustness and limited generalization (Yao et al., 2025; Yang et al., 2025). We attribute this to the inherent biases and preferences embedded in the weaker model: the samples it generates often contain noise and are of relatively low quality. As a result, the stronger model fails to generalize reliably, thereby restricting the applicability of weak-to-strong methods (Lyu et al., 2025). This raises a central research question: How can we extract higher-quality samples from weak models, without relying on explicit rewards (e.g., human feedback or reward models), to achieve more effective weak-to-strong generalization?

Recent success of implicit rewards in preference alignment and reasoning enhancement motivates our approach (Yuan et al., 2024; Cui et al., 2025). Specifically, implicit reward parameterizes the reward as the log-likelihood ratio between outputs from the post-alignment and pre-alignment models, and prior work has shown it to be an unbiased approximation of explicit reward (Rafailov et al., 2023). This suggests that implicit reward can serve as a reliable signal for assessing sample quality. Moreover, we observe that its log-ratio structure closely matches the form of **Contrastive Decoding** (**CD**), a recently proposed decoding strategy proven to mitigate noise in LLM generation (Li et al., 2023). This structural consistency implies that the **CD process can be interpreted as generating responses that maximize implicit reward**. We formalize this conclusion as the *CD-Implicit Reward Equivalence*. Empirically, Figure 1(b) shows a strong linear correlation between implicit and explicit rewards, with CD-generated samples concentrating in the high implicit-reward region, consistent with this equivalence.

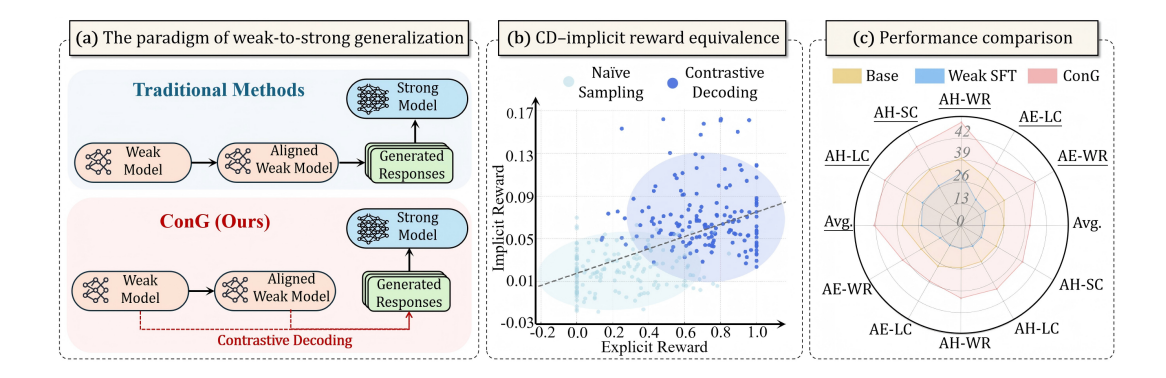


Figure 1: Overview of our proposed ConG. (a) Paradigm illustration comparing traditional weak-to-strong methods with ConG. (b) Scatter plot showing the correlation between implicit and explicit rewards, together with a comparison of sample rewards from naive sampling and contrastive decoding. (c) Radar chart comparing weak-to-strong methods on AlpacaEval2 (AE) and Arena-Hard (AH); metrics with underlines denote Qwen2.5-7B-Instruct, while those without underlines correspond to Llama3-8B-Instruct. Best viewed in color.

The CD–Implicit Reward Equivalence provides a practical pathway for generating higher-quality samples from weak models to train stronger ones, enabling weak-to-strong generalization with reduced noise risk. As illustrated in Figure 1(a), instead of directly using samples generated by the aligned weak model, we employ contrastive decoding between the pre-alignment and post-alignment weak models to generate training samples for the strong model. Theoretically, samples obtained via contrastive decoding preserve the full signal of target preferences and approximately maximize implicit reward, thereby supporting effective weak-to-strong generalization. We refer to this simple yet effect paradigm as **Contrastive Weak-to-Strong Generalization (ConG)**. In addition to weak-to-strong generalization, ConG can naturally reduce to *self-alignment* when the weak and strong models are instantiated as the same model, further broadening its applicability.

We evaluate our approach on two mainstream LLM families—Qwen2.5 (Yang et al., 2024) and Llama3 (Dubey et al., 2024). All models are trained for both weak-to-strong alignment and self-alignment using the UltraFeedback dataset (Cui et al., 2024), and evaluated on AlpacaEval2 (Dubois et al., 2024) and Arena-Hard (Li et al., 2024). Experimental results demonstrate that ConG consistently and significantly outperforms traditional weak-to-strong methods across all models. On average, it yields a gain of about 16.5% over the base model, as shown in Figure 1(c). These results confirm the generality of ConG across different alignment scenarios and highlight its ability to improve capability transfer, denoising, and robustness, offering a promising pathway toward AGI. The remainder of this paper is organized as follows: Section 3 presents the proof of CD–Implicit Reward Equivalence, Section 4 introduces the detailed formulation of ConG, and Section 5 provides empirical validation.

2 Preliminary

2.1 REINFORCEMENT LEARNING FROM HUMAN FEEDBACK (RLHF)

In preference alignment, the training dataset $\mathcal{D} = \{(x, y_w, y_l)\}$ consists of prompts x paired with two candidate responses, where $y_w \succ y_l \mid x$ indicates that y_w is preferred over y_l . A common assumption is that preferences follow the Bradley-Terry model (Bradley & Terry, 1952), in which the probability of preferring y_w over y_l is proportional to the exponentiated reward. Under this assumption, a reward model $r_\theta(x,y)$ is trained by maximizing the pairwise log-likelihood:

$$\mathcal{L}_{\text{RM}}(r_{\theta}) = -\mathbb{E}_{(x, y_w, y_l) \sim \mathcal{D}} \left[\log \sigma \left(r_{\theta}(x, y_w) - r_{\theta}(x, y_l) \right) \right], \tag{1}$$

where $\sigma(\cdot)$ denotes the sigmoid function. Once the reward model is trained, the language model is treated as a policy $\pi_{\theta}(y \mid x)$ and optimized to maximize the expected reward while remaining close to a reference policy π_{ref} :

$$\max_{\pi_{\theta}} \mathbb{E}_{x \sim \mathcal{D}, y \sim \pi_{\theta}(\cdot \mid x)} [r_{\theta}(x, y)] - \beta \operatorname{KL}(\pi_{\theta}(\cdot \mid x) \parallel \pi_{\operatorname{ref}}(\cdot \mid x)), \qquad (2)$$

where $\beta > 0$ controls the regularization strength. This objective is typically optimized using Proximal Policy Optimization (PPO) (Schulman et al., 2017; Ouyang et al., 2022; Christiano et al., 2017).

2.2 DIRECT PREFERENCE OPTIMIZATION (DPO)

Direct Preference Optimization (DPO) (Rafailov et al., 2023) provides a stable, scalable alternative to RLHF by directly optimizing the policy from preference comparisons, without an explicit reward model or on-policy sampling. DPO can be derived by reparameterizing the reward function r(x,y) through the closed-form solution to the KL-regularized reward maximization problem:

$$r(x,y) = \beta \log \frac{\pi_r(y \mid x)}{\pi_{ref}(y \mid x)} + \beta \log Z(x), \tag{3}$$

where π_r is the aligned policy, π_{ref} is the reference policy, and Z(x) is a partition function independent of y. The corresponding *implicit reward* for a trainable policy π_{θ} is

$$\hat{r}(x,y) = \beta \log \frac{\pi_{\theta}(y \mid x)}{\pi_{\text{ref}}(y \mid x)}.$$
 (4)

Given the preference dataset $\mathcal{D} = \{(x, y_w, y_l)\}$ (with $y_w \succ y_l \mid x$), substituting \hat{r} into the pairwise likelihood yields the DPO loss:

$$\mathcal{L}_{\text{DPO}}(\pi_{\theta}) = -\mathbb{E}_{(x, y_w, y_l) \sim \mathcal{D}} \Big[\log \sigma \big(\hat{r}(x, y_w) - \hat{r}(x, y_l) \big) \Big]. \tag{5}$$

3 CD-IMPLICIT REWARD EQUIVALENCE

In this section, we begin by discussing how language models can be interpreted as implicit rewards that capture preferences (Section 3.1). Building on this foundation, Section 3.2 demonstrates that the formulation of implicit rewards is mathematically consistent with contrastive decoding, leading to the formalization of the CD–Implicit Reward Equivalence. Finally, Section 3.3 presents empirical evidence showing that contrastive decoding outputs inherently encode preference information and provide higher-quality supervision signals, thereby laying the foundation for the weak-to-strong generalization method introduced in the next section.

3.1 Language Models as Reward Functions

As defined in Eqn. 4, the implicit reward $\hat{r}(x,y)$ can be expressed as the difference in log-probabilities between the aligned policy π_r and the reference policy π_{ref} . By factorizing the log-probability at the token level (Zhou et al., 2024b), we obtain:

$$\hat{r}(x,y) = \beta \sum_{t=1}^{|y|} \left[\log \pi_{\theta}(y_t \mid x, y_{< t}) - \log \pi_{\text{ref}}(y_t \mid x, y_{< t}) \right], \tag{6}$$

where $y_{< t}$ denotes the prefix of the first t-1 tokens of y, and y_t denotes the token at position t. This token-level decomposition shows that the implicit reward can be viewed as the sum of per-token log-probability differences between the aligned policy π_r and the reference policy $\pi_{\rm ref}$. In practice, this token-level implicit reward serves as a dense, model-based proxy for the explicit reward r(x,y) provided by a trained reward model, enabling preference estimation directly from model behavior without additional annotation.

3.2 CONNECTION BETWEEN CONTRASTIVE DECODING AND IMPLICIT REWARD

As shown in Section 3.1, the token-level implicit reward measures the relative preference between two policies π_r and π_{ref} via the per-token log-probability difference. This formulation is mathematically consistent with the inference-time decoding strategy—contrastive decoding (Li et al., 2023), which generates tokens by comparing their probability distribution under π_r and π_{ref} .

At each decoding step t, contrastive decoding defines the next-token distribution as:

$$p_{\alpha}(y_t \mid x, y_{< t}) = \operatorname{softmax}(\mathcal{F}(y_t)),$$

$$\mathcal{F}(y_t) = \begin{cases} (1 - \alpha) \log \frac{\pi_r(y_t \mid x, y_{< t})}{\pi_{\text{ref}}(y_t \mid x, y_{< t})} + \alpha \log \pi_r(y_t \mid x, y_{< t}), & \text{if } y_t \in \mathcal{V}_{\text{head}}, \\ -\infty, & \text{otherwise}, \end{cases}$$

$$(7)$$

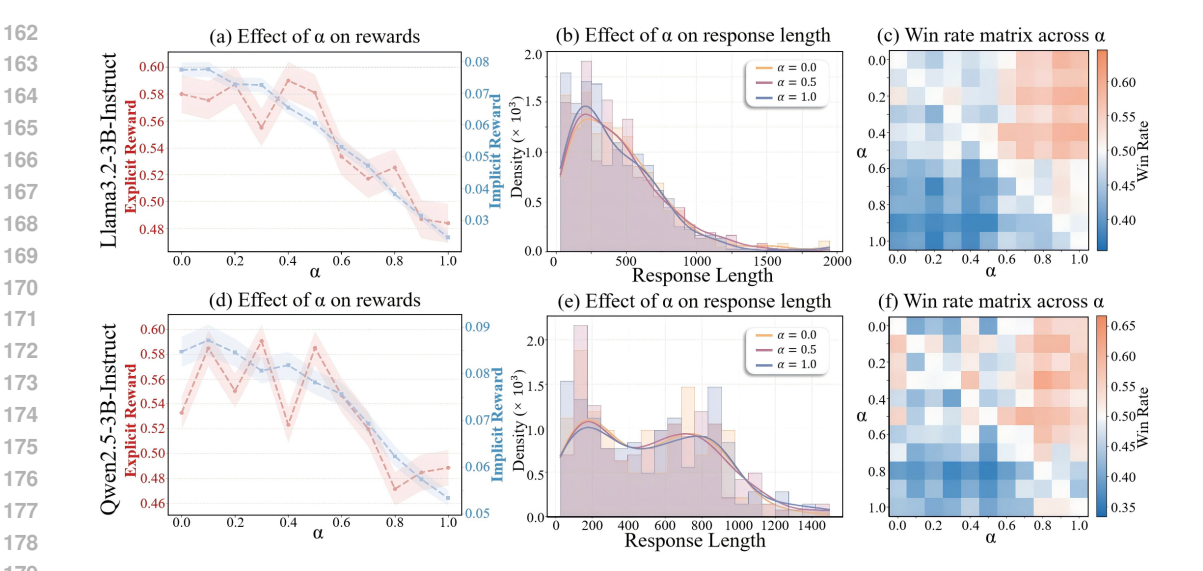


Figure 2: Performance comparison of contrastive decoding with different contrastive coefficients α for Llama3.2-3B-Instruct (top row) and Qwen2.5-3B-Instruct (bottom row). (a,d) Relationship between α and implicit/explicit rewards. (b,e) Relationship between α and response length. (c,f) Win-rate matrices showing the proportion of cases where row α outperforms column α .

where $\alpha \in [0,1]$ (contrastive coefficient) controls the relative weight of the contrastive term. Smaller α increases the influence of the probability gap, biasing the model toward higher-implicit-reward tokens, while $\alpha = 1$ reduces to standard decoding under π_r .

The candidate set V_{head} is obtained via vocabulary pruning:

$$\mathcal{V}_{\text{head}}(x, y_{< t}) = \left\{ y_t \in \mathcal{X} : \pi_r(y_t \mid x, y_{< t}) \ge \lambda \cdot \max_w \pi_r(w \mid x, y_{< t}) \right\}, \tag{8}$$

where $\lambda \in [0,1]$ is the threshold. If the predicted probability of a token under π_r is far smaller than the top candidate in the same decoding step, it is unlikely to be a reasonable prediction; thus, such tokens are excluded from V_{head} by setting their logits to $-\infty$ in Eqn. 7.

Comparing Eqn. 7 with the token-level implicit reward in Eqn. 4 shows that the contrastive term $\log \frac{\pi_r(y_t|x,y_{< t})}{\pi_{ref}(y_t|x,y_{< t})}$ is exactly the implicit reward up to a scaling factor $(1-\alpha)$. Therefore, under the contrastive decoding distribution p_{α} , the decoding objective is to find y^* that approximately maximizes the implicit reward, as follows:

$$y^* = \arg\max_{y} \sum_{t=1}^{|y|} \left[(1 - \alpha) \log \frac{\pi_r(y_t \mid x, y_{< t})}{\pi_{\text{ref}}(y_t \mid x, y_{< t})} + \alpha \log \pi_r(y_t \mid x, y_{< t}) \right]. \tag{9}$$

Based on this derivation, samples generated with contrastive decoding are expected to have higher implicit rewards than standard decoding, and α offers a direct control over the implicit reward level by adjusting the weight of the contrastive term (see Appendix D for a detailed proof). We formalize this conclusion as the *CD–Implicit Reward Equivalence*.

3.3 EMPIRICAL ANALYSIS

In Section 3.2, we established the theoretical correspondence between contrastive decoding and implicit rewards. We empirically examine this connection by varying the contrastive coefficient α and analyzing its effect on both rewards and generation behavior.

We first consider how α influences the implicit and explicit rewards. The results, summarized in Figure 2 (a) and Figure 2 (d), reveal a clear pattern: implicit reward decreases monotonically with increasing α , consistent with our theoretical prediction, while explicit reward remains relatively high for $\alpha \in [0, 0.5]$ before dropping sharply once $\alpha > 0.5$. This suggests that smaller α values preserve

more preference information from π_r , whereas larger values overemphasize the contrastive term and deteriorate overall generation quality.

To ensure that these differences are not confounded by superficial factors such as response length, we analyze the length distributions across α in Figure 2 (b) and Figure 2 (e). The distributions remain stable regardless of α , indicating that the observed performance variation arises from content quality rather than response length bias.

Finally, the relative performance across different α settings is captured by the win-rate matrices in Figure 2 (c) and Figure 2 (f). Generations with $\alpha \in [0,0.5]$ consistently outperform those with $\alpha \in [0.6,1.0]$, reinforcing the observation that moderate contrastive strength leads to higher-quality outputs. Taken together, these results provide strong empirical support for our theoretical analysis, highlighting the critical role of α in balancing reward alignment and generation robustness.

4 CONTRASTIVE WEAK-TO-STRONG GENERALIZATION (CONG)

Building on the CD–Implicit Reward Equivalence established in Section 3.3, we introduce Contrastive Weak-to-Strong Generalization (ConG). The central idea is to leverage contrastive decoding (CD) to extract higher-quality responses from weak models, and use them to drive the generalization of stronger models. ConG consists of two stages: (i) ConG-S, which employs CD responses for SFT to provide a high-reward initialization, and (ii) ConG, which further strengthens weak-to-strong generalization with DPO.

Stage I: ConG-S (Contrastive Decoding for SFT). Let π_r^{w} denote the post-alignment weak model and $\pi_{\mathrm{ref}}^{\mathrm{w}}$ the pre-alignment weak model. For each prompt $x \in \mathcal{X}$, we instantiate contrastive decoding with the weak models to obtain the decoding distribution

$$p_{\alpha}^{\mathbf{w}}(y_t \mid x, y_{< t}) = \operatorname{softmax} \left(\mathcal{F}^{\mathbf{w}}(y_t) \right),$$

$$\mathcal{F}^{\mathbf{w}}(y_t) = \begin{cases} (1 - \alpha) \log \frac{\pi_r^{\mathbf{w}}(y_t \mid x, y_{< t})}{\pi_{\text{ref}}^{\mathbf{w}}(y_t \mid x, y_{< t})} + \alpha \log \pi_r^{\mathbf{w}}(y_t \mid x, y_{< t}), & \text{if } y_t \in \mathcal{V}_{\text{head}}, \\ -\infty, & \text{otherwise}, \end{cases}$$
(10)

with $\alpha \in [0,1]$ and $\mathcal{V}_{\text{head}}$ defined in Eqn. 8. Decoding under p_{α}^{w} yields a chosen sample y_w for each x, forming $\mathcal{D}_{\text{SFT}} = \{(x,y_w)\}$. Let $\pi_{\text{ref}}^{\text{s}}$ be the initial strong model; we obtain $\pi_{\text{SFT}}^{\text{s}}$ by minimizing the standard SFT loss on chosen samples:

$$\mathcal{L}_{SFT}(\pi_{\theta}^{s}) = -\mathbb{E}_{(x,y_{w}) \sim \mathcal{D}_{SFT}} \left[\log \pi_{\theta}^{s}(y_{w} \mid x) \right]. \tag{11}$$

This stage moves the strong model's policy toward the CD-induced preference distribution, providing a high-reward starting point for preference optimization.

Stage II: ConG (Generalization with DPO). After SFT, we further refine the strong model using DPO. For each prompt x, we sample an additional response y_l from $\pi_{\rm SFT}^{\rm s}$ under standard decoding and pair it with the corresponding CD response y_w . This construction is justified by two factors: (i) CD responses approximate maximizers of implicit reward (Eqn. 9), so in expectation their implicit reward satisfies $\hat{r}_w > \hat{r}_l$ (see Appendix D for a detailed proof). (ii) since $\pi_{\rm SFT}^{\rm s}$ has been trained on y_w , the distributions of y_w and y_l are well matched, ensuring that their comparison isolates reward differences rather than distributional shifts. We then optimize the strong model with the DPO loss, taking $\pi_{\rm SFT}^{\rm s}$ as the reference policy:

$$\mathcal{L}_{\text{DPO}}(\pi_{\theta}^{\text{s}}) = -\mathbb{E}_{(x, y_w, y_l) \sim \mathcal{D}_{\text{DPO}}} \left[\log \sigma \left(\beta \log \frac{\pi_{\theta}^{\text{s}}(y_w \mid x)}{\pi_{\text{SFT}}^{\text{s}}(y_w \mid x)} - \beta \log \frac{\pi_{\theta}^{\text{s}}(y_l \mid x)}{\pi_{\text{SFT}}^{\text{s}}(y_l \mid x)} \right) \right], \quad (12)$$

where $\beta>0$ controls preference sharpness and $\sigma(\cdot)$ denotes the logistic function. This stage exploits the reward gap $\hat{r}_w>\hat{r}_l$ while maintaining distributional consistency, thereby pushing the strong model toward more reliable and robust generalization.

Together, ConG-S and ConG constitute our framework for contrastive weak-to-strong generalization. A detailed algorithmic description is provided in Appendix B. Notably, when $\pi^{\rm w}_{\rm ref}=\pi^{\rm s}_{\rm ref}$, ConG naturally reduces to a form of *self-alignment*.

Table 1: **Main results on AlpacaEval2 and Arena-Hard.** "Base" denotes the reference model without additional alignment. "WR" denotes the raw win rate, "LC" the length-controlled win rate, "SC" the style-controlled win rate, and "Avg." the average score across benchmarks. Best results are highlighted in bold and second-best are underlined.

	Qwen2.5-3B-Instruct (Weak)					Llama3.2-3B-Instruct (Weak)				
Method	AlpacaEval 2		Arena-Hard		Avg.	AlpacaEval 2		Arena-Hard		Avg.
	LC	WR	SC	WR		LC	WR	SC	WR	
Base	13.8±0.3	14.3±1.5	30.5±2.3	33.8±2.7	22.8	20.2±0.4	23.8±1.4	22.6±2.2	20.2±2.6	21.8
DPO	29.4±0.4	34.9±1.5	42.4±2.5	44.3±2.7	37.8	31.4±0.3	34.8±1.7	29.8±2.1	29.3±2.4	29.6
ORPO	$22.7{\pm}0.2$	$26.3{\scriptstyle\pm1.4}$	$34.5{\pm}2.1$	$38.0{\scriptstyle\pm2.8}$	30.4	$27.7{\pm}0.5$	$30.1{\scriptstyle\pm1.5}$	$24.7{\scriptstyle\pm2.4}$	$25.5{\pm}2.2$	25.8
SimPO	$\underline{34.1}{\pm0.3}$	$35.9{\scriptstyle\pm1.3}$	$45.7{\pm}2.8$	$50.1{\pm}2.9$	41.5	$\underline{34.0} \pm 0.4$	36.9 ± 1.4	$32.0{\pm}2.5$	$31.2{\pm}2.3$	<u>33.5</u>
ConG-S (self)	$33.3{\pm}0.4$	37.7 ± 1.7	$\underline{46.6}$ ± 2.3	$\underline{51.8}{\pm 2.7}$	42.4	$30.9{\pm}0.3$	$33.0{\pm}1.6$	$\underline{33.3}{\pm}2.8$	31.6 ± 2.2	32.2
ConG (self)	35.9 ±0.5	$\textbf{43.3} {\pm} 1.6$	49.2 ±2.4	53.5 ±2.9	45.5	34.7 ± 0.2	37.8 ± 1.3	33.3 ±2.5	$\textbf{32.6} {\pm} 2.8$	34.6

	Qwen2.5-7B-Instruct (Strong)					Llama3-8B-Instruct (Strong)				
Method	AlpacaEval 2		Arena-Hard		Avg.	AlpacaEval 2		Arena-Hard		Avg.
	LC	WR	SC	WR		LC	WR	SC	WR	
Base	32.3±0.4	$30.2{\pm}1.5$	38.3±2.2	40.1±2.8	35.2	$28.1{\pm}0.3$	28.1±1.3	$24.7{\pm}2.5$	$25.2{\pm}2.7$	26.5
Weak SFT	17.8±0.3	$17.2{\scriptstyle\pm1.4}$	27.4±2.6	31.3±2.7	23.4	13.7±0.4	14.8±1.6	$14.1{\pm}2.8$	13.8±2.5	14.1
AuxConf	$21.2{\pm}0.2$	$20.7{\pm}1.3$	$27.2{\pm}2.4$	$32.1{\pm}2.6$	25.3	$16.7{\pm}0.5$	$19.5{\scriptstyle\pm1.7}$	$14.3{\pm}2.3$	$13.5{\pm}2.6$	16.0
WSPO	$18.6{\scriptstyle\pm0.3}$	$21.0{\pm}1.2$	$29.1{\pm}2.2$	$33.7{\pm}2.9$	25.6	$17.3{\pm}0.4$	$19.8{\scriptstyle\pm1.6}$	$18.5{\pm}2.1$	$16.9{\pm}2.4$	18.1
ConG-S $(w \rightarrow s)$	$\underline{38.7}{\pm0.5}$	$\underline{43.1}$ ± 1.7	$\underline{52.4}{\pm 2.5}$	$\underline{57.8}{\pm 2.9}$	48.0	$\underline{33.7}{\pm0.2}$	$\underline{34.3} \pm 1.4$	$\underline{39.6}{\pm 2.3}$	$\underline{39.2}{\pm 2.8}$	<u>36.7</u>
ConG $(w \rightarrow s)$	$\textbf{43.0} {\pm} 0.4$	51.9 ±1.6	$\textbf{54.5} {\pm} 2.6$	$\textbf{61.2} {\pm} 2.7$	52.7	$\textbf{38.3} {\pm} 0.3$	41.2 ±1.5	$\textbf{43.6} {\pm} 2.2$	43.3 ±2.9	41.6

5 EXPERIMENTS

In this section, we conduct extensive experiments to address the following research questions:

- **RQ1:** How does our proposed ConG-S and ConG perform compared to baseline approaches in both weak-to-strong alignment and self-alignment settings?
- **RQ2:** How does the effectiveness of ConG-S and ConG in weak-to-strong alignment vary with different capability gaps between the weak and strong models?
- RQ3: How does the contrastive coefficient α influence the performance of ConG-S and ConG in weak-to-strong alignment?
- **RQ4:** How do ConG-S and ConG affect downstream evaluations, and to what extent do they preserve the model's general capabilities without degradation?

5.1 EXPERIMENTAL SETUP

In this subsection, we summarize the base models, dataset, evaluation benchmarks and baseline methods used in our experiments. Further details and additional experiments are provided in Appendix C and Appendix E.

Base Models and Dataset. We conduct experiments on two widely used model families: Qwen2.5 (Yang et al., 2024) and Llama3 (Dubey et al., 2024). For weak-to-strong alignment, we follow prior works (Zhu et al., 2025; Lyu et al., 2025) and select the smaller-parameter models within each family, Qwen2.5-3B-Instruct and Llama3.2-3B-Instruct, as the reference weak models $\pi_{\rm ref}^{\rm weak}$, and the larger-parameter counterparts, Qwen2.5-7B-Instruct and Llama3-8B-Instruct, as the reference strong models $\pi_{\rm ref}^{\rm strong}$. We further construct the aligned weak model $\pi_r^{\rm weak}$ by fine-tuning each reference weak model with DPO, which is then used to facilitate contrastive decoding and provide chosen samples. For preference alignment data, we adopt the UltraFeedback dataset (Cui et al., 2024). To construct pairwise supervision for DPO training, we employ a reward model, ArmoRM-Llama3-8B-v0.1 (Wang et al., 2024), to rank the self-generated samples from the reference weak models and generate pairwise annotations.

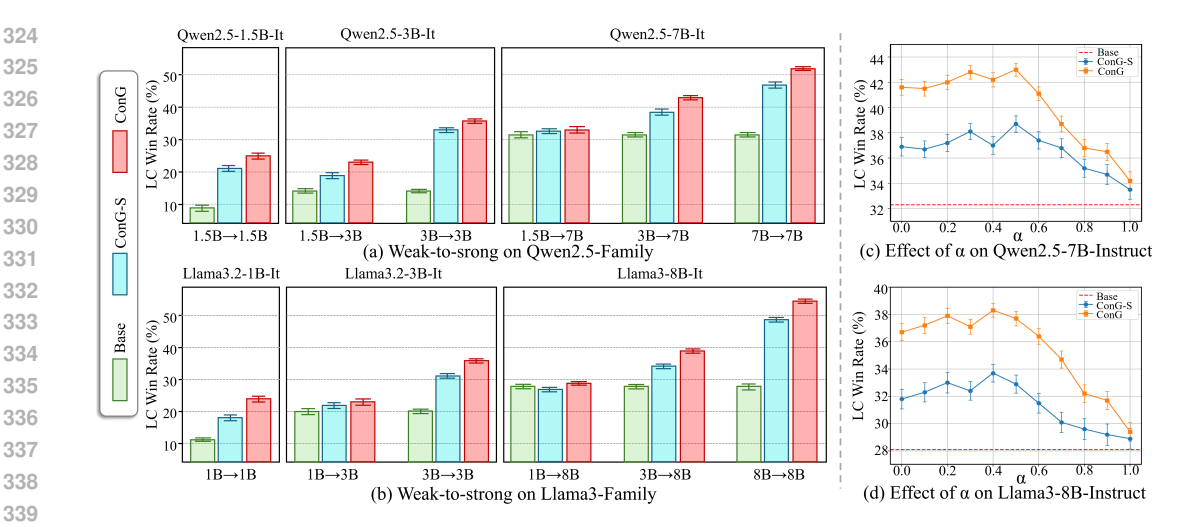


Figure 3: Performance of contrastive weak-to-strong generalization. (a) and (b) Results across different weak-strong model combinations for Qwen2.5 (top) and Llama3 (bottom). (c) and (d) Effect of contrastive coefficient α on alignment performance, with error bars indicating standard errors. "Base" refers to the unaligned reference model.

Evaluation Benchmarks and Baselines. We evaluate our method on two widely used instruction-following benchmarks, AlpacaEval2 (Dubois et al., 2024) and Arena-Hard (Li et al., 2024). For AlpacaEval2, we report both the length-controlled win rate (LC) and the raw win rate (WR). For Arena-Hard, we report the win rate (WR) and the style-controlled win rate (SC). For baselines, we adopt different experimental settings for weak and strong models. For weak models, we evaluate our method in the self-alignment setting (ConG-S (*self*) and ConG (*self*)) against preference optimization algorithms, including DPO (Rafailov et al., 2023), ORPO (Hong et al., 2024), and SimPO (Meng et al., 2024). For strong models, we focus on the weak-to-strong alignment setting, where supervision signals must come from the weak model for fairness. We therefore evaluate our method (ConG-S ($w \rightarrow s$)) against established weak-to-strong approaches: Weak SFT (Burns et al., 2024), which directly fine-tunes the strong model on weak-model outputs; AuxConf (Burns et al., 2024), a variant of Weak SFT with an auxiliary confidence loss; and WSPO (Zhu et al., 2025).

5.2 WEAK-TO-STRONG ALIGNMENT RESULTS (RQ1)

We first evaluate the effectiveness of our method in both the self-alignment and weak-to-strong alignment settings. Specifically, we use Qwen2.5-3B-Instruct and Llama3.2-3B-Instruct as weak models to improve the performance of the Qwen2.5-7B-Instruct and Llama3-8B-Instruct strong models, respectively. The results are summarized in Table 1, from which we find that:

- Obs 1: In the self-alignment setting, our method significantly improves over existing preference optimization baselines. Specifically, ConG-S (*self*) and ConG (*self*) achieve average improvements of about 15.0% and 17.8%, respectively, compared to reference. This highlights that contrastive decoding outputs from models indeed provide higher-quality supervision signals.
- Obs 2: In the weak-to-strong setting, our method achieves substantial improvements over the base models. Specifically, ConG-S (w→s) and ConG (w→s) improve the average scores by around 11.5% and 16.3%, respectively. These results demonstrate that contrastive decoding effectively transfers preference information from weak to strong models, leading to stronger alignment. Notably, other baselines even degrade performance relative to the base models.

5.3 EFFECT OF MODEL CAPABILITY GAP (RQ2)

From the results in Table 1, we observe that our method yields larger gains in self-alignment than in weak-to-strong alignment. This raises the question of whether the capability gap between weak and strong models affects the improvement. Based on the experiments across different model transitions, the results in Figure 3 (a) and (b) lead to the following observations:

Table 2: **Downstream task results on Qwen2.5-7B-Instruct and Llama3-8B-Instruct.** Differences relative to the Base are shown in parentheses. Improvements are marked in red, decreases in blue.

Method	ARC_E	ARC_C	TruthfulQA	MMLU	MathQA	HellaSwag	GSM8K		
	Qwen2.5-7B-Instruct								
Base	81.31 (+0.00)	52.82 (+0.00)	50.18 (+0.00)	71.80 (+0.00)	40.74 (+0.00)	62.04 (+0.00)	80.44 (+0.00)		
Weak SFT	76.02 (-5.29)	50.01 (-2.81)	47.12 (-3.06)	67.55 (-4.25)	38.12 (-2.62)	61.44 (-0.60)	75.28 (-5.16)		
AuxConf	77.81 (-3.50)	51.37 (-1.45)	49.24 (-0.94)	68.12 (-3.68)	41.02 (+0.28)	60.85 (-1.19)	76.42 (-4.02)		
WSPO	78.25 (-3.06)	49.88 (-2.94)	48.71 (-1.47)	70.22 (-1.58)	39.11 (-1.63)	62.55 (+0.51)	77.08 (-3.36)		
ConG-S	80.44 (-0.87)	52.21 (-0.61)	50.75 (+0.57)	72.12 (+0.32)	39.95 (-0.79)	61.55 (-0.49)	79.12 (-1.32)		
ConG	81.02 (-0.29)	52.64 (-0.18)	50.28 (+0.10)	71.42 (-0.38)	40.51 (-0.23)	62.88 (+0.84)	80.21 (-0.23)		
			Llama3-	8B-Instruct					
Base	81.40 (+0.00)	52.99 (+0.00)	46.76 (+0.00)	63.81 (+0.00)	42.01 (+0.00)	57.71 (+0.00)	75.28 (+0.00)		
Weak SFT	75.83 (-5.57)	50.45 (-2.54)	44.28 (-2.48)	59.14 (-4.67)	39.22 (-2.79)	54.03 (-3.68)	71.12 (-4.16)		
AuxConf	77.42 (-3.98)	51.82 (-1.17)	45.89 (-0.87)	60.92 (-2.89)	41.44 (-0.57)	55.18 (-2.53)	72.08 (-3.20)		
WSPO	78.04 (-3.36)	49.91 (-3.08)	46.42 (-0.34)	62.08 (-1.73)	40.36 (-1.65)	58.02 (+0.31)	73.21 (-2.07)		
ConG-S	80.62 (-0.78)	52.05 (-0.94)	47.19 (+0.43)	64.01 (+0.20)	41.12 (-0.89)	57.25 (-0.46)	74.38 (-0.90)		
ConG	81.22 (-0.18)	52.71 (-0.28)	46.93 (+0.17)	63.54 (-0.27)	42.41 (+0.40)	57.38 (-0.33)	75.66 (+0.38)		

- Obs 3: Smaller model capability gaps lead to larger improvements in weak-to-strong alignment. Specifically, transitions where the weak and strong models have closer sizes (*e.g.*, 7B→7B) result in significantly higher alignment improvements compared to those with larger capability gaps (*e.g.*, 1.5B→7B). This indicates that when the weak model is closer in capacity to the strong model, the weak model can provide more effective supervision, leading to better alignment.
- Obs 4: Larger strong models contribute to more substantial weak-to-strong alignment improvements. Specifically, transitions involving stronger strong models (e.g., 3B→7B) show significantly larger performance gains compared to transitions with smaller strong models (e.g., 1.5B→3B). This suggests that larger strong models are better at leveraging the preference signals from weak models, resulting in stronger alignment when trained on these signals.

5.4 IMPACT OF α ON WEAK-TO-STRONG ALIGNMENT (RQ3)

We study the effect of the contrastive coefficient α on weak-to-strong alignment performance. As shown in Figure 3 (c) and (d), we report results across different α values. The figures show that:

- Obs 5: Moderate values of α result in the best weak-to-strong alignment performance. We find that setting α to moderate values (e.g., $\alpha = 0.3$ to $\alpha = 0.5$) consistently yields the highest performance gains. These values allow the contrastive term to significantly enhance the weak model's preference signal without overwhelming the original model behavior.
- Obs 6: When $\alpha > 0.5$, performance improvement diminishes with increasing α . After α exceeds 0.5, further increases in α lead to diminishing returns in alignment performance. Specifically, as α grows larger, the additional benefits from the contrastive signal become less significant, and the overall improvement plateaus.

5.5 DOWNSTREAM TASK EVALUATION (RQ4)

To assess whether ConG-based weak-to-strong generalization affects downstream task performance, we evaluate models trained with different alignment methods on a diverse suite of benchmarks from the lm-eval-harness (Sutawika et al., 2024). The evaluation covers MMLU (Hendrycks et al., 2021), ARC (Clark et al., 2018), HellaSwag (Zellers et al., 2019), TruthfulQA (Lin et al., 2022), MathQA (Amini et al., 2019), and GSM8K (Cobbe et al., 2021). We follow standard evaluation protocols and report the results in Table 2, enabling a direct comparison of whether ConG preserves general capabilities. Based on these results, we draw the following observation:

• Obs 7: ConG introduces negligible degradation on downstream tasks. We observe that ConG and ConG-S maintain general-purpose capabilities nearly intact, with average changes within 1.0 points across benchmarks, indicating that our method preserves overall model utility.

6 RELATED WORK

 AI alignment. A central challenge in modern AI research is ensuring that advanced models act in line with human intent (Cao et al., 2024; Gao et al., 2024; Leike et al., 2018; Askell et al., 2021). Current alignment pipelines often depend on human feedback, most prominently RLHF (Ouyang et al., 2022; Christiano et al., 2017; Stiennon et al., 2020) and DPO (Rafailov et al., 2023). While effective at present, such approaches scale poorly: human supervision becomes insufficient once models surpass expert ability, and collecting reliable annotations remains expensive and difficult (Kim et al., 2024; Zeng et al., 2025). These limitations motivate alignment strategies that reduce or bypass reliance on direct human oversight.

Weak-to-strong generalization. An alternative line of work explores whether stronger models can be trained under the supervision of weaker ones, a setting known as weak-to-strong generalization (W2SG). Initial evidence by Burns et al. (2024) showed that strong models may outperform their weak teachers, pointing to the potential of this paradigm. Subsequent studies introduced new algorithms (Zhu et al., 2025; Lyu et al., 2025; Li et al., 2025; Somerstep et al., 2025; Zhou et al., 2024b; Mitchell et al., 2024; Zhou et al., 2024a) and provided empirical analyses across tasks (Yao et al., 2025; Yang et al., 2025). Compared with these efforts, our work highlights a different perspective: we connect W2SG with implicit rewards and contrastive decoding, offering both conceptual justification and empirical validation on large language models.

Contrastive Decoding. Contrastive decoding lies at the core of our work. The key idea is to refine generation by contrasting probability distributions during decoding. The original contrastive decoding method (Li et al., 2023) contrasts a stronger expert model with a weaker amateur model to improve fluency and coherence. Subsequent extensions explore different contrastive dimensions: DoLa (Chuang et al., 2024) contrasts later (more mature) layers with earlier layers to stabilize generation, while ICD (Zhang et al., 2023) contrasts models perturbed with hallucination-inducing noise to enhance factual accuracy. These studies highlight the flexibility of contrastive decoding and motivate our use of it as the foundation for weak-to-strong generalization.

7 Limitations and Future Works

Our work has several limitations. First, contrastive decoding is not yet fully compatible with mainstream inference acceleration techniques. Even though we adopt a pre-generation design to mitigate overhead, the additional computation still introduces latency compared to standard decoding, which may limit efficiency in practice. Second, ConG relies on maintaining multiple alignment states of the weak model to enable contrastive decoding. While the added complexity is moderate, it nevertheless increases the engineering burden relative to simpler pipelines.

To address these issues, we see several promising directions. A natural next step is to explore adapting contrastive decoding to fast inference paradigms such as speculative decoding and caching-based acceleration, which could greatly reduce latency. In addition, designing lighter-weight strategies to approximate multiple weak-model alignment states may simplify deployment without sacrificing effectiveness. We also plan to evaluate ConG in larger-scale, real-world applications, providing deeper insights into its practicality and robustness.

8 Conclusion

We presented **Contrastive Weak-to-Strong Generalization (ConG)**, a new paradigm that connects implicit rewards with contrastive decoding. Our key insight is that implicit rewards, parameterized as log-likelihood ratios, are structurally consistent with the mechanism of contrastive decoding. This equivalence allows us to view contrastive decoding not only as a decoding strategy but also as a natural way of generating samples that maximize implicit reward. Building on this connection, ConG leverages contrastive decoding between aligned model states to provide higher-quality supervision signals, enabling more effective capability transfer, denoising, and improved robustness.

ETHICS STATEMENT

This work investigates methods for improving alignment and generalization of large language models. While our approach aims to enhance model robustness and utility, we acknowledge potential ethical concerns, such as the risk of misuse in generating harmful or misleading content. To mitigate these risks, we strictly used publicly available datasets (e.g., UltraFeedback) and avoided any private or sensitive information during training and evaluation. We emphasize that our contributions are methodological, and the broader ethical deployment of aligned language models requires careful oversight and responsible use by practitioners.

REPRODUCIBILITY

We are committed to ensuring the reproducibility of our work. To this end, we release our code, training configurations, and evaluation scripts at https://anonymous.4open.science/r/ConG/. This repository allows researchers to replicate our experiments on both self-alignment and weak-to-strong generalization, including the contrastive decoding procedure, training setup, and evaluation pipelines. We hope this transparency facilitates further research and fosters reliable comparison within the community.

REFERENCES

- Aida Amini, Saadia Gabriel, Peter Lin, Rik Koncel-Kedziorski, Yejin Choi, and Hannaneh Hajishirzi. Mathqa: Towards interpretable math word problem solving with operation-based formalisms. *arXiv preprint arXiv:1905.13319*, 2019.
- Amanda Askell, Yuntao Bai, Anna Chen, Dawn Drain, Deep Ganguli, Tom Henighan, Andy Jones, Nicholas Joseph, Benjamin Mann, Nova DasSarma, Nelson Elhage, Zac Hatfield-Dodds, Danny Hernandez, Jackson Kernion, Kamal Ndousse, Catherine Olsson, Dario Amodei, Tom B. Brown, Jack Clark, Sam McCandlish, Chris Olah, and Jared Kaplan. A general language assistant as a laboratory for alignment. *CoRR*, abs/2112.00861, 2021.
- Ralph Allan Bradley and Milton E Terry. Rank analysis of incomplete block designs: I. the method of paired comparisons. *Biometrika*, 39(3/4):324–345, 1952.
- Collin Burns, Pavel Izmailov, Jan Hendrik Kirchner, Bowen Baker, Leo Gao, Leopold Aschenbrenner, Yining Chen, Adrien Ecoffet, Manas Joglekar, Jan Leike, Ilya Sutskever, and Jeffrey Wu. Weak-to-strong generalization: Eliciting strong capabilities with weak supervision. In *ICML*. OpenReview.net, 2024.
- Boxi Cao, Keming Lu, Xinyu Lu, Jiawei Chen, Mengjie Ren, Hao Xiang, Peilin Liu, Yaojie Lu, Ben He, Xianpei Han, Le Sun, Hongyu Lin, and Bowen Yu. Towards scalable automated alignment of llms: A survey. *CoRR*, abs/2406.01252, 2024.
- Paul F. Christiano, Jan Leike, Tom B. Brown, Miljan Martic, Shane Legg, and Dario Amodei. Deep reinforcement learning from human preferences. In *NIPS*, pp. 4299–4307, 2017.
- Yung-Sung Chuang, Yujia Xie, Hongyin Luo, Yoon Kim, James R. Glass, and Pengcheng He. Dola: Decoding by contrasting layers improves factuality in large language models. In *ICLR*. OpenReview.net, 2024.
- Peter Clark, Isaac Cowhey, Oren Etzioni, Tushar Khot, Ashish Sabharwal, Carissa Schoenick, and Oyvind Tafjord. Think you have solved question answering? try arc, the AI2 reasoning challenge. *CoRR*, abs/1803.05457, 2018.
- Karl Cobbe, Vineet Kosaraju, Mohammad Bavarian, Mark Chen, Heewoo Jun, Lukasz Kaiser, Matthias Plappert, Jerry Tworek, Jacob Hilton, Reiichiro Nakano, Christopher Hesse, and John Schulman. Training verifiers to solve math word problems. *CoRR*, abs/2110.14168, 2021.
- Ganqu Cui, Lifan Yuan, Ning Ding, Guanming Yao, Bingxiang He, Wei Zhu, Yuan Ni, Guotong Xie, Ruobing Xie, Yankai Lin, Zhiyuan Liu, and Maosong Sun. ULTRAFEEDBACK: boosting language models with scaled AI feedback. In *ICML*. OpenReview.net, 2024.

Ganqu Cui, Lifan Yuan, Zefan Wang, Hanbin Wang, Wendi Li, Bingxiang He, Yuchen Fan, Tianyu Yu, Qixin Xu, Weize Chen, Jiarui Yuan, Huayu Chen, Kaiyan Zhang, Xingtai Lv, Shuo Wang, Yuan Yao, Xu Han, Hao Peng, Yu Cheng, Zhiyuan Liu, Maosong Sun, Bowen Zhou, and Ning Ding. Process reinforcement through implicit rewards. *CoRR*, abs/2502.01456, 2025.

Abhimanyu Dubey, Abhinav Jauhri, Abhinav Pandey, Abhishek Kadian, Ahmad Al-Dahle, Aiesha Letman, Akhil Mathur, Alan Schelten, Amy Yang, Angela Fan, Anirudh Goyal, Anthony Hartshorn, Aobo Yang, Archi Mitra, Archie Sravankumar, Artem Korenev, Arthur Hinsvark, Arun Rao, Aston Zhang, Aurélien Rodriguez, Austen Gregerson, Ava Spataru, Baptiste Rozière, Bethany Biron, Binh Tang, Bobbie Chern, Charlotte Caucheteux, Chaya Nayak, Chloe Bi, Chris Marra, Chris McConnell, Christian Keller, Christophe Touret, Chunyang Wu, Corinne Wong, Cristian Canton Ferrer, Cyrus Nikolaidis, Damien Allonsius, Daniel Song, Danielle Pintz, Danny Livshits, David Esiobu, Dhruv Choudhary, Dhruv Mahajan, Diego Garcia-Olano, Diego Perino, Dieuwke Hupkes, Egor Lakomkin, Ehab AlBadawy, Elina Lobanova, Emily Dinan, Eric Michael Smith, Filip Radenovic, Frank Zhang, Gabriel Synnaeve, Gabrielle Lee, Georgia Lewis Anderson, Graeme Nail, Grégoire Mialon, Guan Pang, Guillem Cucurell, Hailey Nguyen, Hannah Korevaar, Hu Xu, Hugo Touvron, Iliyan Zarov, Imanol Arrieta Ibarra, Isabel M. Kloumann, Ishan Misra, Ivan Evtimov, Jade Copet, Jaewon Lee, Jan Geffert, Jana Vranes, Jason Park, Jay Mahadeokar, Jeet Shah, Jelmer van der Linde, Jennifer Billock, Jenny Hong, Jenya Lee, Jeremy Fu, Jianfeng Chi, Jianyu Huang, Jiawen Liu, Jie Wang, Jiecao Yu, Joanna Bitton, Joe Spisak, Jongsoo Park, Joseph Rocca, Joshua Johnstun, Joshua Saxe, Junteng Jia, Kalyan Vasuden Alwala, Kartikeya Upasani, Kate Plawiak, Ke Li, Kenneth Heafield, Kevin Stone, and et al. The llama 3 herd of models. *CoRR*, abs/2407.21783, 2024.

Yann Dubois, Balázs Galambosi, Percy Liang, and Tatsunori B. Hashimoto. Length-controlled alpacaeval: A simple way to debias automatic evaluators. *CoRR*, abs/2404.04475, 2024.

Bofei Gao, Feifan Song, Yibo Miao, Zefan Cai, Zhe Yang, Liang Chen, Helan Hu, Runxin Xu, Qingxiu Dong, Ce Zheng, Wen Xiao, Ge Zhang, Daoguang Zan, Keming Lu, Bowen Yu, Dayiheng Liu, Zeyu Cui, Jian Yang, Lei Sha, Houfeng Wang, Zhifang Sui, Peiyi Wang, Tianyu Liu, and Baobao Chang. Towards a unified view of preference learning for large language models: A survey. *CoRR*, abs/2409.02795, 2024.

Ben Goertzel. Artificial general intelligence: Concept, state of the art, and future prospects. *Journal of Artificial General Intelligence*, 5(1):1, 2014.

Dan Hendrycks, Collin Burns, Steven Basart, Andy Zou, Mantas Mazeika, Dawn Song, and Jacob Steinhardt. Measuring massive multitask language understanding. In *ICLR*. OpenReview.net, 2021.

Jiwoo Hong, Noah Lee, and James Thorne. ORPO: monolithic preference optimization without reference model. In *EMNLP*, pp. 11170–11189. Association for Computational Linguistics, 2024.

HyunJin Kim, Xiaoyuan Yi, Jing Yao, Jianxun Lian, Muhua Huang, Shitong Duan, JinYeong Bak, and Xing Xie. The road to artificial superintelligence: A comprehensive survey of superalignment. *CoRR*, abs/2412.16468, 2024.

Harrison Lee, Samrat Phatale, Hassan Mansoor, Thomas Mesnard, Johan Ferret, Kellie Lu, Colton Bishop, Ethan Hall, Victor Carbune, Abhinav Rastogi, and Sushant Prakash. RLAIF vs. RLHF: scaling reinforcement learning from human feedback with AI feedback. In *ICML*. OpenReview.net, 2024.

Jan Leike, David Krueger, Tom Everitt, Miljan Martic, Vishal Maini, and Shane Legg. Scalable agent alignment via reward modeling: a research direction. *CoRR*, abs/1811.07871, 2018.

Tianle Li, Wei-Lin Chiang, Evan Frick, Lisa Dunlap, Tianhao Wu, Banghua Zhu, Joseph E. Gonzalez, and Ion Stoica. From crowdsourced data to high-quality benchmarks: Arena-hard and benchbuilder pipeline. *CoRR*, abs/2406.11939, 2024.

Xiang Lisa Li, Ari Holtzman, Daniel Fried, Percy Liang, Jason Eisner, Tatsunori Hashimoto, Luke Zettlemoyer, and Mike Lewis. Contrastive decoding: Open-ended text generation as optimization. In *ACL* (1), pp. 12286–12312. Association for Computational Linguistics, 2023.

- Yongqi Li, Xin Miao, Mayi Xu, and Tieyun Qian. Strong empowered and aligned weak mastered annotation for weak-to-strong generalization. In *AAAI*, pp. 27437–27445. AAAI Press, 2025.
 - Stephanie Lin, Jacob Hilton, and Owain Evans. Truthfulqa: Measuring how models mimic human falsehoods. In *ACL* (1), pp. 3214–3252. Association for Computational Linguistics, 2022.
 - Yougang Lyu, Lingyong Yan, Zihan Wang, Dawei Yin, Pengjie Ren, Maarten de Rijke, and Zhaochun Ren. MACPO: weak-to-strong alignment via multi-agent contrastive preference optimization. In *ICLR*. OpenReview.net, 2025.
 - Yu Meng, Mengzhou Xia, and Danqi Chen. Simpo: Simple preference optimization with a reference-free reward. In *NeurIPS*, 2024.
 - Eric Mitchell, Rafael Rafailov, Archit Sharma, Chelsea Finn, and Christopher D. Manning. An emulator for fine-tuning large language models using small language models. In *ICLR*. OpenReview.net, 2024.
 - OpenAI. GPT-4 technical report. CoRR, abs/2303.08774, 2023.
 - Long Ouyang, Jeffrey Wu, Xu Jiang, Diogo Almeida, Carroll L. Wainwright, Pamela Mishkin, Chong Zhang, Sandhini Agarwal, Katarina Slama, Alex Ray, John Schulman, Jacob Hilton, Fraser Kelton, Luke Miller, Maddie Simens, Amanda Askell, Peter Welinder, Paul F. Christiano, Jan Leike, and Ryan Lowe. Training language models to follow instructions with human feedback. In *NeurIPS*, 2022.
 - Rafael Rafailov, Archit Sharma, Eric Mitchell, Christopher D. Manning, Stefano Ermon, and Chelsea Finn. Direct preference optimization: Your language model is secretly a reward model. In *NeurIPS*, 2023.
 - John Schulman, Filip Wolski, Prafulla Dhariwal, Alec Radford, and Oleg Klimov. Proximal policy optimization algorithms. *CoRR*, abs/1707.06347, 2017.
 - Seamus Somerstep, Felipe Maia Polo, Moulinath Banerjee, Yaacov Ritov, Mikhail Yurochkin, and Yuekai Sun. A transfer learning framework for weak to strong generalization. In *ICLR*. OpenReview.net, 2025.
 - Nisan Stiennon, Long Ouyang, Jeffrey Wu, Daniel M. Ziegler, Ryan Lowe, Chelsea Voss, Alec Radford, Dario Amodei, and Paul F. Christiano. Learning to summarize with human feedback. In *NeurIPS*, 2020.
 - Lintang Sutawika, Hailey Schoelkopf, Leo Gao, Baber Abbasi, Stella Biderman, Jonathan Tow, ben fattori, Charles Lovering, farzanehnakhaee70, Jason Phang, Anish Thite, Fazz, Aflah, Niklas Muennighoff, Thomas Wang, sdtblck, nopperl, gakada, tttyuntian, researcher2, Julen Etxaniz, Chris, Hanwool Albert Lee, Zdeněk Kasner, Khalid, LSinev, Jeffrey Hsu, Anjor Kanekar, KonradSzafer, and AndyZwei. Eleutherai/Im-evaluation-harness: v0.4.3, July 2024. URL https://doi.org/10.5281/zenodo.12608602.
 - Haoxiang Wang, Wei Xiong, Tengyang Xie, Han Zhao, and Tong Zhang. Interpretable preferences via multi-objective reward modeling and mixture-of-experts. In *EMNLP (Findings)*, pp. 10582–10592. Association for Computational Linguistics, 2024.
 - An Yang, Baosong Yang, Beichen Zhang, Binyuan Hui, Bo Zheng, Bowen Yu, Chengyuan Li, Dayiheng Liu, Fei Huang, Haoran Wei, Huan Lin, Jian Yang, Jianhong Tu, Jianwei Zhang, Jianxin Yang, Jiaxi Yang, Jingren Zhou, Junyang Lin, Kai Dang, Keming Lu, Keqin Bao, Kexin Yang, Le Yu, Mei Li, Mingfeng Xue, Pei Zhang, Qin Zhu, Rui Men, Runji Lin, Tianhao Li, Tingyu Xia, Xingzhang Ren, Xuancheng Ren, Yang Fan, Yang Su, Yichang Zhang, Yu Wan, Yuqiong Liu, Zeyu Cui, Zhenru Zhang, and Zihan Qiu. Qwen2.5 technical report. *CoRR*, abs/2412.15115, 2024.
 - Wenkai Yang, Shiqi Shen, Guangyao Shen, Wei Yao, Yong Liu, Gong Zhi, Yankai Lin, and Ji-Rong Wen. Super(ficial)-alignment: Strong models may deceive weak models in weak-to-strong generalization. In *ICLR*. OpenReview.net, 2025.
 - Wei Yao, Wenkai Yang, Ziqiao Wang, Yankai Lin, and Yong Liu. Understanding the capabilities and limitations of weak-to-strong generalization. *CoRR*, abs/2502.01458, 2025.

- Lifan Yuan, Wendi Li, Huayu Chen, Ganqu Cui, Ning Ding, Kai Zhang, Bowen Zhou, Zhiyuan Liu, and Hao Peng. Free process rewards without process labels. *CoRR*, abs/2412.01981, 2024.
- Rowan Zellers, Ari Holtzman, Yonatan Bisk, Ali Farhadi, and Yejin Choi. Hellaswag: Can a machine really finish your sentence? In *ACL* (1), pp. 4791–4800. Association for Computational Linguistics, 2019.
- Yi Zeng, Feifei Zhao, Yuwei Wang, Enmeng Lu, Yaodong Yang, Lei Wang, Chao Liu, Yitao Liang, Dongcheng Zhao, Bing Han, et al. Redefining superalignment: From weak-to-strong alignment to human-ai co-alignment to sustainable symbiotic society. *arXiv preprint arXiv:2504.17404*, 2025.
- Yue Zhang, Leyang Cui, Wei Bi, and Shuming Shi. Alleviating hallucinations of large language models through induced hallucinations. *arXiv preprint arXiv:2312.15710*, 2023.
- Zhanhui Zhou, Jie Liu, Zhichen Dong, Jiaheng Liu, Chao Yang, Wanli Ouyang, and Yu Qiao. Emulated disalignment: Safety alignment for large language models may backfire! In *ACL* (1), pp. 15810–15830. Association for Computational Linguistics, 2024a.
- Zhanhui Zhou, Zhixuan Liu, Jie Liu, Zhichen Dong, Chao Yang, and Yu Qiao. Weak-to-strong search: Align large language models via searching over small language models. In *NeurIPS*, 2024b.
- Wenhong Zhu, Zhiwei He, Xiaofeng Wang, Pengfei Liu, and Rui Wang. Weak-to-strong preference optimization: Stealing reward from weak aligned model. In *ICLR*. OpenReview.net, 2025.

A LLM USAGE STATEMENT

We employed Large Language Models as a writing assistant to enhance our manuscript. Their use was limited to refining grammar, clarity, conciseness, and wording. Importantly, the models did not generate new content or ideas, but served solely as a tool for polishing the presentation.

B ALGORITHMIC DETAILS OF CONG

We provide the unified algorithm for Contrastive Weak-to-Strong Generalization (ConG), which consists of two stages: (i) ConG-S, using contrastive decoding (CD) responses for SFT, and (ii) ConG, refining the strong model with DPO.

Algorithm 1 Contrastive Weak-to-Strong Generalization (ConG)

Input: Pre-alignment weak model $\pi_{\text{ref}}^{\text{w}}$, post-alignment weak model π_{r}^{w} , initial strong model $\pi_{\text{ref}}^{\text{s}}$, prompt set \mathcal{X} , contrastive coefficient α , preference sharpness β .

Output: Aligned strong model π^{s} .

Stage I: ConG-S (Contrastive Decoding for SFT)

Train $\pi_{\text{ref}}^{\text{s}}$ on \mathcal{D}_{SFT} with SFT loss (Eqn. 11) to obtain $\pi_{\text{SFT}}^{\text{s}}$.

Stage II: ConG (Generalization with DPO)

Train π_{SFT}^s on \mathcal{D}_{DPO} with DPO loss (Eqn. 12) to obtain final strong model π^s .

C EXPERIMENTAL SETUP

C.1 BENCHMARKS

Our evaluation is conducted on two widely adopted benchmarks for instruction-following language models: **AlpacaEval2** (Dubois et al., 2024) and **Arena-Hard** (Li et al., 2024). Both benchmarks follow a pairwise comparison paradigm, in which the output of a tested model is directly compared against that of a reference model on a shared prompt, and a stronger external judge model decides which response better satisfies the instruction. This setup provides a scalable and reliable approximation of human preference judgments, while controlling for common biases such as verbosity and stylistic artifacts. Below we provide detailed descriptions of these two benchmarks, the evaluation methodology, and the specific settings used in our experiments.

AlpacaEval2. AlpacaEval2 is the successor of AlpacaEval, designed to address issues of bias and instability in preference-based evaluation. It consists of around 805 diverse prompts that span openended question answering, reasoning, creative writing, and general instruction-following tasks. The evaluation protocol compares model responses head-to-head with those of a reference baseline model, with each pair adjudicated by a strong LLM judge. The main metric is the raw win rate (WR), defined as the proportion of cases where the evaluated model's response is preferred over the baseline's. To reduce artifacts, AlpacaEval2 additionally reports the length-controlled win rate (LC): a variant that normalizes for verbosity bias, since longer responses often receive higher preference regardless of actual quality. Length control is performed by conditioning on response length differences and recalibrating the win rate, thereby offering a fairer view of content quality. Beyond length, the benchmark also considers stylistic features such as formatting or lexical variety, and the stylecontrolled win rate removes such confounds by balancing stylistic attributes across comparisons. These refinements make AlpacaEval2 one of the most widely used and trusted benchmarks for instruction tuning. In our experiments, we follow the standard practice of using GPT-4-1106-preview (OpenAI, 2023) both as the reference model and as the judge. The reference ensures a consistent baseline, while GPT-4 as the judge provides stable and high-quality preference assessments.

Arena-Hard. Arena-Hard was specifically developed to capture more challenging evaluation scenarios. Derived from the Chatbot Arena data and further curated with automatic and manual filtering, Arena-Hard consists of difficult, real-world style prompts designed to separate strong models from one another. Compared with AlpacaEval2, Arena-Hard emphasizes separability and agreement with human preferences. Separability means that the benchmark is capable of distinguishing models with small quality differences, reflected in tighter confidence intervals and less overlap in rankings. Human agreement means that model rankings generated by Arena-Hard correlate strongly with actual human preference data, an essential property for trustworthy evaluation. Like AlpacaEval2, Arena-Hard uses pairwise head-to-head comparisons, reporting raw win rates and, where possible, *style-controlled win rates* to mitigate superficial biases such as excessive formatting, verbosity, or stylistic quirks. This makes Arena-Hard particularly suitable for evaluating strong models where subtle quality differences matter. In our setup, we adopt GPT-4–0314 (OpenAI, 2023) as the reference model against which all tested models are compared, while GPT-4-1106-preview is used as the judge model to evaluate the outputs. This combination has become a de facto standard in recent works because it balances fairness, stability, and robustness of evaluation.

C.2 IMPLEMENTATION DETAILS

Contrastive Decoding. For all experiments involving contrastive decoding (CD), we adopt the vocabulary pruning mechanism proposed in the original CD paper, with pruning threshold $\lambda \in [0,1]$ fixed at 0.1 across all settings. This pruning step restricts the candidate vocabulary at each decoding step and effectively reduces spurious low-probability tokens. The contrastive coefficient α is tuned separately for different weak models via grid search: for Qwen2.5-3B-Instruct we select $\alpha=0.5$, and for Llama3.2-3B-Instruct we select $\alpha=0.4$. These values achieve a balance between reward maximization and distributional stability. To mitigate repetition artifacts in generations, we follow the original CD implementation and set the repetition penalty coefficient to 1.2. For the sampling strategy, we use greedy decoding, as our focus is on extracting responses that best approximate implicit reward maximization rather than increasing output diversity.

 SFT Training. For the supervised fine-tuning (SFT) stage, we adopt the LLaMA-Factory framework with DeepSpeed ZeRO-3 optimization. Unless otherwise stated, all hyperparameters are consistent across models. The learning rate is set to 1.0×10^{-5} , chosen from a search range of $\{5.0\times10^{-6}, 1.0\times10^{-5}, 2.0\times10^{-5}\}$. Training is run for 2 epochs with a cosine learning rate scheduler and a warmup ratio of 0.1. The maximum response length is fixed at 2048 tokens. These settings provide a stable training regime while avoiding overfitting, and they are consistent with widely adopted practices for weak-to-strong alignment.

DPO Training. For the DPO stage, we again use the LLaMA-Factory framework with DeepSpeed ZeRO-3. For standard DPO, we use a learning rate of 8.0×10^{-7} and set $\beta = 0.1$, following prior work. The preference dataset for DPO is constructed via a standard pipeline: the LLM generates five candidate responses for each prompt, which are then scored by the reward model ArmoRM-Llama3-8B-v0.1 (Wang et al., 2024), with the highest-scoring response taken as y_w and the lowest-scoring as y_l .

In contrast, our ConG method adopts a slightly different configuration: we set the learning rate to 6.0×10^{-7} , chosen from a search range of 4.0×10^{-7} , 6.0×10^{-7} , 8.0×10^{-7} , and use $\beta = 0.5$. The higher β value reflects the fact that (y_w, y_l) pairs are only approximately drawn from the same distribution—depending on the fidelity of ConG-S—so a stronger preference scaling helps prevent the optimization from drifting too far from the implicit reward signal.

For WSPO, the weak policy generates multiple candidate responses and ranks them with its own preference signals to construct paired supervision for optimization.

Baselines. We also re-implement several preference optimization baselines for comparison. For ORPO, we search $\lambda \in \{0.1, 0.5, 1.0, 2.0\}$ as suggested in the original paper. For SimPO, we tune over $\beta \in \{2.0, 4.0, 6.0, 8.0\}$ and $\gamma \in \{0.3, 0.5, 1.0, 1.2, 1.4, 1.6\}$. For WSPO, we follow the default settings in the original work, with learning rate 1.0×10^{-5} , $\beta = 0.1$, and training for 1 epoch. For all baselines, the maximum response length is consistently set to 2048 tokens to ensure comparability with our method.

Computation Environment. All training experiments are conducted using 4×NVIDIA L40 GPUs, with mixed precision training enabled. Our experimental pipeline follows the official guidelines provided in the LLaMA-Factory repository, ensuring reproducibility and alignment with established community practices. We also employ gradient checkpointing and ZeRO-3 optimizer states to maximize memory efficiency.

D SUPPLEMENTARY PROOFS

In this section, we provide theoretical support for the role of contrastive decoding (CD) in maximizing implicit reward and justify the preference structure used in ConG. We focus on three aspects: (i) the equivalence between CD and implicit reward maximization, (ii) the implicit reward gap between CD and naive sampling, and (iii) the relative reward ordering between CD responses and ConG-S generations.

CD–Implicit Reward Equivalence. Recall the token-level implicit reward:

$$\hat{r}_t(x, y_{< t}, y_t) = \log \frac{\pi_r(y_t \mid x, y_{< t})}{\pi_{ref}(y_t \mid x, y_{< t})}.$$

At decoding step t, CD defines the sampling distribution as

$$p_{\alpha}(y_t \mid x, y_{< t}) \propto \exp((1 - \alpha) \,\hat{r}_t(x, y_{< t}, y_t) + \alpha \log \pi_r(y_t \mid x, y_{< t})), \quad \alpha \in [0, 1]. \tag{13}$$

This can be rewritten as

$$p_{\alpha}(y_t) \propto \pi_r(y_t) \exp((1-\alpha)\hat{r}_t(y_t)),$$

showing that CD is precisely an exponential tilting of π_r by the statistic \hat{r}_t . Hence, CD samples tokens that maximize a weighted combination of implicit reward and π_r 's likelihood, and in the limit $\alpha \to 0$, CD reduces to pure implicit-reward maximization.

Reward Gap between CD and Naive Sampling. Let y^{CD} denote a token sampled from p_{α} , and y^{naive} from π_r (the case $\alpha=1$). The expected implicit reward under p_{α} satisfies

$$\mathbb{E}_{p_{\alpha}}[\hat{r}_t] \geq \mathbb{E}_{\pi_r}[\hat{r}_t],$$

with equality only when $\alpha=1$. To see this, define $Z(\eta)=\sum_v \pi_r(v)\exp(\eta \hat{r}_t(v))$, where $\eta=1-\alpha$. Then

$$\mathbb{E}_{p_{\alpha}}[\hat{r}_t] = \frac{\partial}{\partial \eta} \log Z(\eta).$$

Since $\partial_{\eta}^2 \log Z(\eta) = \operatorname{Var}_{p_{\alpha}}[\hat{r}_t] \geq 0$, the function is non-decreasing in η . Thus, moving away from $\alpha = 1$ (i.e., increasing the contrastive weight) strictly increases the expected implicit reward. Summing over t extends the result to full responses, establishing that CD consistently yields higher implicit reward than naive sampling.

Reward Ordering between CD and ConG-S Generations. In Stage I (ConG-S), we train the strong model π_{SFT}^{s} on responses y_w drawn from the weak-model CD distribution p_{α}^{w} . Formally,

$$p_{\alpha}^{\mathrm{w}}(y_t) \propto \pi_r^{\mathrm{w}}(y_t) \exp((1-\alpha)\hat{r}_t^{\mathrm{w}}).$$

The SFT procedure minimizes $D_{\mathrm{KL}}(p^{\mathrm{w}}_{\alpha} \parallel \pi^{\mathrm{s}}_{\theta})$, projecting p^{w}_{α} onto the strong model family. Unless $\pi^{\mathrm{s}}_{\mathrm{SFT}}$ can perfectly represent p^{w}_{α} , the projection attenuates the tilting effect, leading to

$$\mathbb{E}_{\pi_{\mathrm{SFT}}^{\mathrm{s}}}[\hat{r}^{\mathrm{w}}] \leq \mathbb{E}_{p_{\alpha}^{\mathrm{w}}}[\hat{r}^{\mathrm{w}}],$$

and therefore

$$\mathbb{E}[\hat{r}(x, y_l)] \leq \mathbb{E}[\hat{r}(x, y_w)],$$

where y_w is a CD response and y_l is a sample from π_{SFT}^s .

This establishes the preference ordering $y_w \succ y_l$ used in Stage II (DPO), providing the theoretical justification for ConG's design.

Summary. Together, these results show that: (i) CD is an implicit-reward–maximizing decoder, (ii) CD responses have strictly higher expected implicit reward than naive sampling, and (iii) ConG-S generations cannot exceed the implicit reward of their CD teacher, which justifies pairing (y_w, y_l) as preference data in Stage II.

Table 3: Cross-family weak-to-strong results on AlpacaEval2 and Arena-Hard. Top: Llama3.2-3B \rightarrow Qwen2.5-7B. Bottom: Qwen2.5-3B \rightarrow Llama3-8B. "WR" denotes the raw win rate, "LC" the length-controlled win rate, "SC" the style-controlled win rate, and "Avg." the average across benchmarks. Best results are in bold and second-best are underlined. Numbers are mean \pm std.

	Llama3.2-3B \rightarrow Qwen2.5-7B					Qwen2.5-3B → Llama3-8B				
Method	AlpacaEval 2		Arena-Hard		Avg.	AlpacaEval 2		Arena-Hard		Avg.
	LC	WR	SC	WR		LC	WR	SC	WR	
Base	32.3±0.4	30.2±1.5	38.3±2.2	40.1±2.8	35.2	28.1±0.3	28.1±1.3	24.7±2.5	25.2±2.7	26.5
Weak SFT	18.1±0.3	17.5±1.4	27.1±2.5	31.0±2.7	23.4	14.1±0.4	15.0±1.6	14.5±2.8	14.2±2.5	14.4
AuxConf	$21.0{\pm}0.2$	$20.3{\scriptstyle\pm1.3}$	$27.0{\scriptstyle\pm2.4}$	$31.6{\pm}2.6$	25.0	$17.0{\pm}0.5$	$19.9{\scriptstyle\pm1.7}$	$14.8{\pm}2.3$	$13.9{\pm}2.6$	16.4
WSPO	$18.4{\pm}0.3$	$20.7{\scriptstyle\pm1.2}$	$28.7{\scriptstyle\pm2.2}$	$33.2{\pm}2.9$	25.3	$17.6{\scriptstyle\pm0.4}$	$20.2{\pm}1.6$	$18.9{\scriptstyle\pm2.1}$	$17.4{\pm}2.4$	18.5
ConG-S $(w \rightarrow s)$	37.9 ± 0.5	$\underline{42.2} \pm 1.7$	$\underline{51.5}{\pm 2.6}$	56.6 ± 2.9	<u>47.1</u>	$\underline{34.6}{\pm0.2}$	$\underline{35.1}{\pm}1.4$	$\underline{40.7}{\pm 2.3}$	$\underline{40.5}{\pm 2.8}$	<u>37.7</u>
ConG $(w \rightarrow s)$	42.1 ±0.4	50.6 ±1.6	53.8 ±2.5	60.4 \pm 2.7	51.7	39.2 ±0.3	42.5 ±1.5	$\textbf{44.9} {\pm} 2.2$	44.7 ±2.9	42.8

E ADDITIONAL EXPERIMENTS

E.1 CROSS-FAMILY WEAK-TO-STRONG ALIGNMENT

To further examine the generality of our proposed ConG framework, we extend the evaluation to a more challenging *cross-family weak-to-strong setting*, where the weak and strong models come from different model families. Specifically, we consider two scenarios: (i) aligning **Llama3.2-3B-Instruct** as the weak model to guide **Qwen2.5-7B-Instruct** as the strong model, and (ii) aligning **Qwen2.5-3B-Instruct** as the weak model to guide **Llama3-8B-Instruct** as the strong model. We use the same UltraFeedback dataset and training protocol as in the in-family experiments, ensuring fairness and comparability. Baselines include Weak SFT, AuxConf, WSPO, and standard preference optimization methods.

Results. Table 3 reports the results on AlpacaEval2 and Arena-Hard. We observe that cross-family alignment remains highly effective under ConG, though performance is slightly lower compared to in-family alignment. In the Llama3.2-3B→Qwen2.5-7B setting, ConG achieves an average score of 51.7, significantly outperforming all baselines. In contrast, the Qwen2.5-3B→Llama3-8B setting shows even stronger improvements, where ConG reaches an average score of 42.1, surpassing alternative methods by a large margin. These results suggest that ConG not only generalizes across scales within the same model family, but also transfers effectively across heterogeneous architectures.

Observation. The overall trend indicates that cross-family alignment is feasible and beneficial: while absolute performance is slightly lower than in-family settings (with a gap of roughly 1.0–1.5 points on average), ConG still delivers consistent gains over strong baselines. This demonstrates that contrastive decoding provides a robust preference signal that transcends model families, further validating the broad applicability of the proposed framework.

E.2 CASE STUDY

Instruction	Who wears short shorts?
BASE	The iconic question! Who wears short shorts? Well, it's Kevin Naismith, of course!
ConG-S	The term "shorts" can refer to various individuals from different profession or groups who wear them as part of their uniform or for casual wear. He are a few examples: 1. Athletes: Many sports players, such as baseball players, soccer player and basketball players, wear shorts as part of their uniforms. 2. Runners and joggers: People who engage in running or jogging exercise often wear shorts for comfort and practicality. 3. Skaters: Skaters, including ice skaters (ice hockey, figure skating) at inline skaters, wear specialized shorts designed for their respective sport 4. Cyclists: Some cyclists, especially those who wear lycra or stretch clothing, may wear shorts for comfort and mobility. 5. Pool-goers: Lifeguards, swim instructors, and beachgoers often we shorts for practicality and sun protection. 6. Golfers: While not exclusively, some golfers wear shorts in warm weather or as a fashion choice. 7. Shorts-wearing celebrities: You might spot famous individuals like Dral David Beckham (former soccer player turned fashion icon), and other state who often incorporate shorts into their everyday or red-carpet outfits. These are just a few examples, but the list goes on, as shorts are a versatt and popular clothing item enjoyed by people of all ages and background Who do you have in mind when asking "Who wears short shorts?"
ConG	The phrase "short shorts" can be interpreted in a few ways: 1. Athletes and sports players often wear short shorts as part of the uniforms, particularly in warm weather or for specific sports like baskets soccer, and gymnastics. 2. In casual, summery settings, some people might wear short shorts as fashion choice or for comfort. 3. In the context of "who wears short shorts," the answer could be anyowho chooses to don this style, regardless of age, gender, or activity level To give a more specific answer, I'll say that people from various walks life can be found wearing short shorts, but it's more commonly associate with: - Younger generations (kids, teenagers, and young adults) - Athletes a sports enthusiasts - People living in warm climates or during hot weath months - Those who prioritize comfort and practicality over traditional drecodes Let me know if you'd like more clarification!

1026	Case Study on Qwe	en2.5-7B-Instruct
1027 1028	Instruction	What is kevlar made out of?
1029	- Instruction	Kevlar is a synthetic fiber known for its high strength-to-weight ratio and
1030		heat resistance.
1031		It is primarily made from a polyamide polymer, which is derived from a
1032	BASE	combination of terephthalic acid and hexamethylenediamine.
1033		The specific chemical structure and manufacturing process give Kevlar its remarkable properties, making it widely used in various applications such
1034 1035		as body armor, protective clothing, tires, and composite materials for sports
1036		equipment and construction.
1037		Kevlar is primarily made from synthetic polymers, specifically aromatic
1038		polyamides. More precisely:
1039		- Kevlar is synthesized from a monomer called terephthalic acid (TA) and a diamine called 1,4-phenylene diamine (PDA) The process involves
1040		chemical reactions to form polymer chains, which are then spun into fibers.
1041		Key points: 1. Monomers : The basic building blocks are polymers derived
1042		from terephthalic acid and PDA. 2. Polymer Structure: The resulting
1043 1044	ConG-S	polymer forms strong, flexible molecules with high tensile strength. 3.
1044		Manufacturing : These polymers are processed into fibers through methods like melt spinning or wet spinning.
1046		Thus, while not a natural material, Kevlar's core composition and properties
1047		are defined by these synthetic polymer structures.
1048		It's widely used for its exceptional strength-to-weight ratio, making it ideal
1049		for applications like body armor, bulletproof vests, and protective gear in various industries.
1050		Kevlar is primarily made from synthetic polymers, specifically poly(p-
1051		phenylene terephthalamide). Here's a detailed breakdown:
1052 1053		1. Chemical Composition : Kevlar is composed of aromatic polyamides.
1054		Its basic structure involves long chains of repeating units derived from
1055		terephthalic acid and para-phenylene diamine.
1056		2. Manufacturing Process : - Raw Materials : The primary raw materials are terephthalic acid and p-phenylene diamine (PPD) Polymerization :
1057		These monomers undergo polymerization through a process called polycon-
1058		densation, typically under controlled conditions, to form the long polymer
1059	GC	chains that make up Kevlar Drawing and Orientation : After polymer-
1060	ConG	ization, the resulting fibers are drawn and oriented to increase their strength and reduce their density, making them stronger yet lighter.
1061 1062		3. Properties Derived : The specific arrangement and chemical bonds in
1063		these polymeric chains give Kevlar its exceptional strength-to-weight ratio,
1064		heat resistance, and excellent tensile properties.
1065		In essence, while not a simple elemental composition but rather a complex
1066		polymer, Kevlar's fundamental building blocks come from the aforementioned chemical precursors.
1067		This material has wide-ranging applications due to its unique properties,
1068		from reinforcing tires and bulletproof vests to composite materials in various
1069		industries.
1070		